Supplementary information

The Role of Mn in Boosting Wide Potential Window on Solid Solution Derived Electrodes for Aqueous Supercapacitors

Ziying Shi,[ab] Enzuo Liu,[a] Biao Chen,[ab] Junwei Sha,[a] Lihua Qian,[c] Zhijia Zhang,[d] Xiaopeng Han,[ab] Wenbin Hu,[ab] Chunnian He,[ab] Naiqin Zhao[ab] and Jianli Kang[ab]*

a School of Materials Science and Engineering, Tianjin University, Tianjin, 300350, P.R. China.

b National Industry-Education Platform of Energy Storage, Tianjin University, 135 Yaguan Road, Tianjin, 300350, P.R. China.

c School of Physics, Huazhong University of Science and Technology, Wuhan, 430074, P.R. China.

d School of Materials Science and Engineering, Tiangong University, Tianjin, 300387, P.R. China.

1. Calculation of capacitance

The volumetric specific capacitance from the GCD curves could calculate based on Equations (S1):

$$C_v = \frac{I \cdot \Delta t}{V \cdot \Delta U} \tag{S1}$$

where C_v was the volumetric specific capacitance (F cm^{-3}), k was the CV scan rate (mV s^{-1}), V was the working volume of the electrode (cm^3), ΔU was the working potential window (V), I was the current (A), and Δt was the discharge time (s).

The volumetric specific capacitance of the SSC device from the GCD curves was calculated from Equation (S2):

$$F_v = \frac{I \cdot \Delta t}{V \cdot \Delta U} \tag{S2}$$

where F_v was the volumetric specific capacitance of the device (F cm^{-3}), I was the current (A), V was the volume of the device (cm^3), ΔU was the working voltage (V) and Δt was the discharge time (s). The volumetric energy density (E_v, mWh cm^{-3}) and volumetric power density (P_v, mW cm^{-3}) were calculated by the following Equations (S3) and (S4):

$$E_v = \frac{F_v \cdot \Delta U^2}{2 \times 3600} \tag{S3}$$

$$P_v = \frac{3600 \cdot E_v}{\Delta t} \tag{S4}$$

2. Supporting Figures

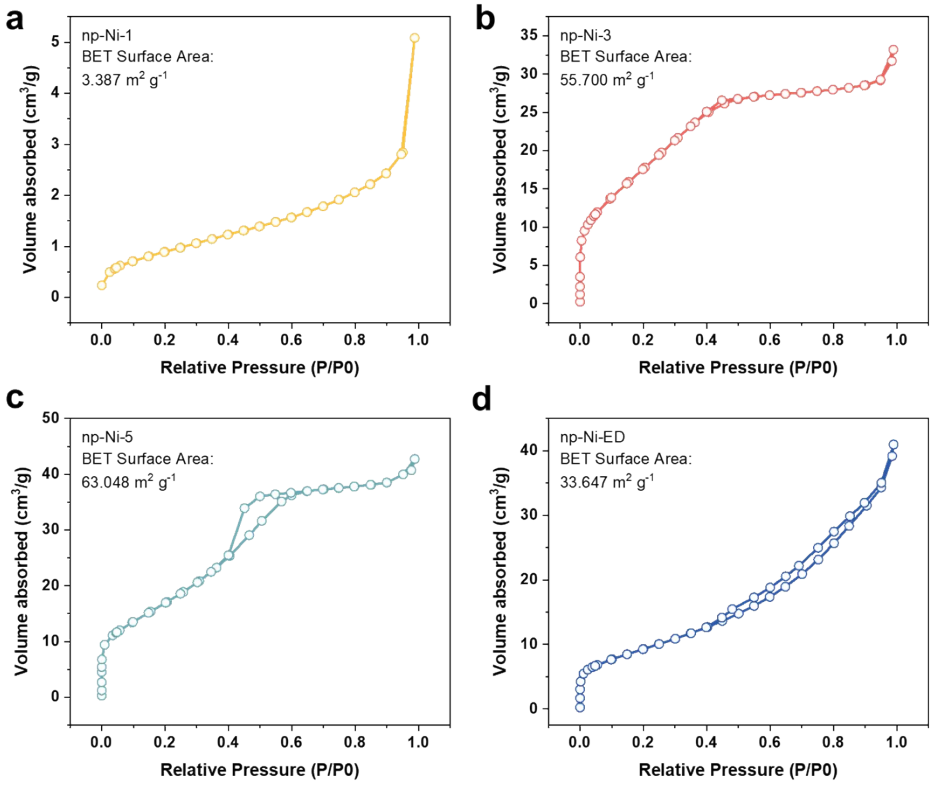

Figure S1. Nitrogen adsorption-desorption isotherm results of (a-c) np-Ni-X (X=1, 3, 5) and (d) np-Ni-ED.

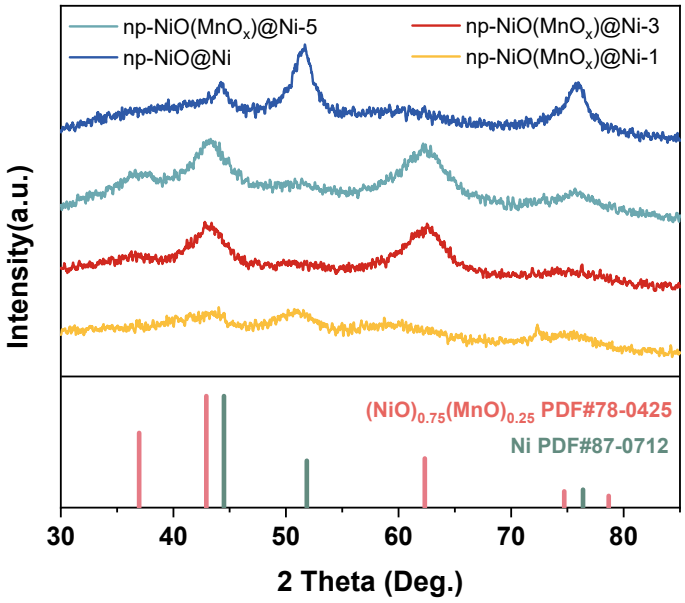

Figure S2. XRD patterns of np-NiO(MnO_x)@Ni-X (X=1, 3, and 5) and np-NiO@Ni.

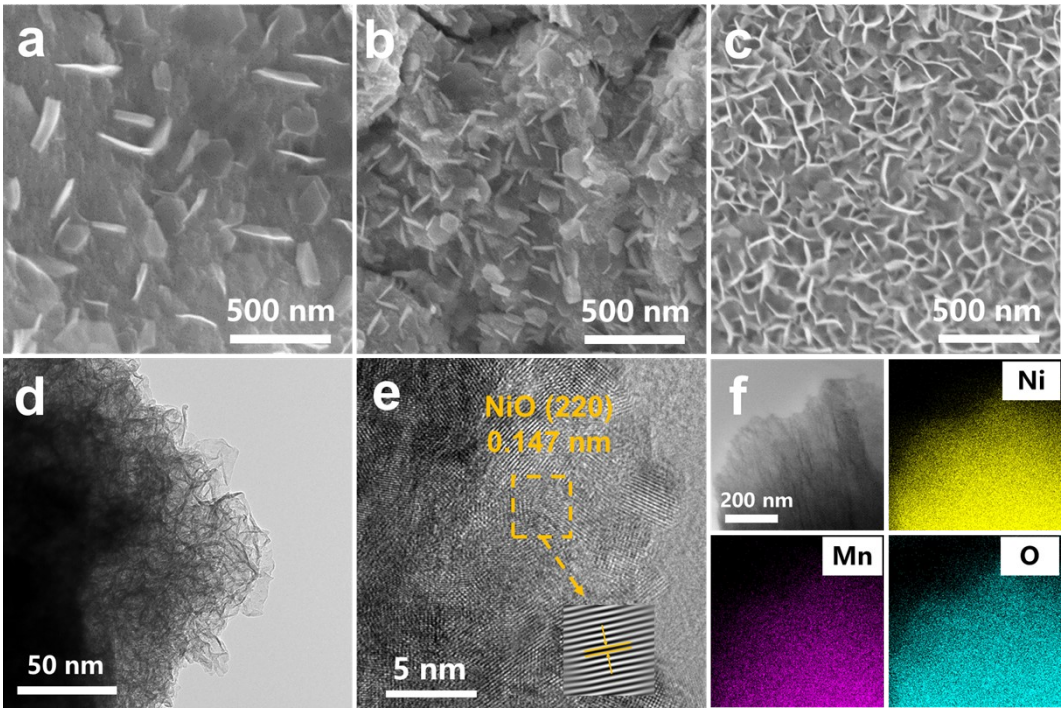

Figure S3. (a-b) The structure of np-Ni-5 after polarization treatment; (c) The SEM image of np-NiO(MnO_x)@Ni-5; (d) TEM image of np-NiO(MnO_x)@Ni-5 (f) HRTEM image of np-NiO(MnO_x)@Ni-5. (f) The EDS element mapping images of np-NiO(MnO_x)@Ni-5 for a selected region.

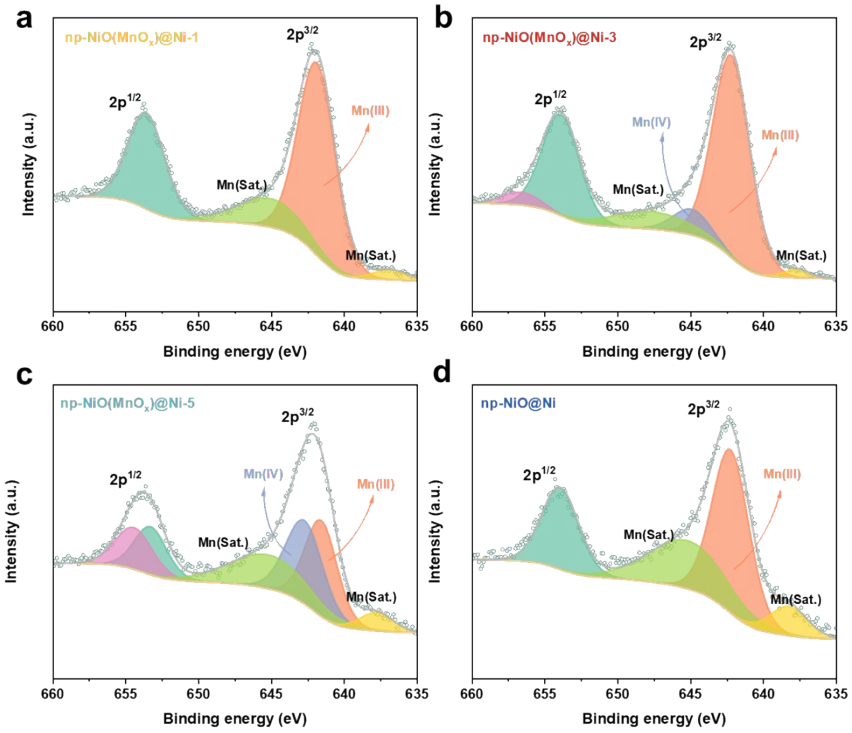

Figure S4. XPS high-resolution spectra of Mn 2p in (a) np-NiO(MnO_x)@Ni-1, (b) np-NiO(MnO_x)@Ni-3, (c) np-NiO(MnO_x)@Ni-5 and (d) np-NiO@Ni.

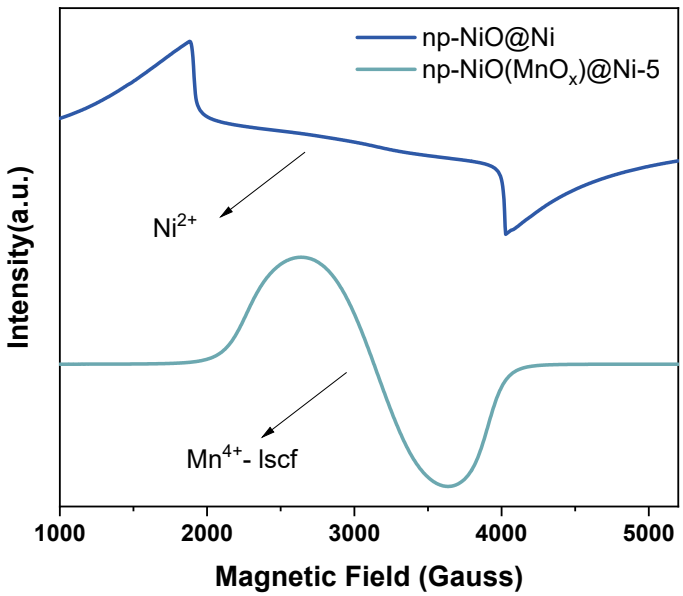

Figure S5. The ESR spectra for np-NiO(MnO_x)@Ni-5 and np-NiO@Ni electrodes.

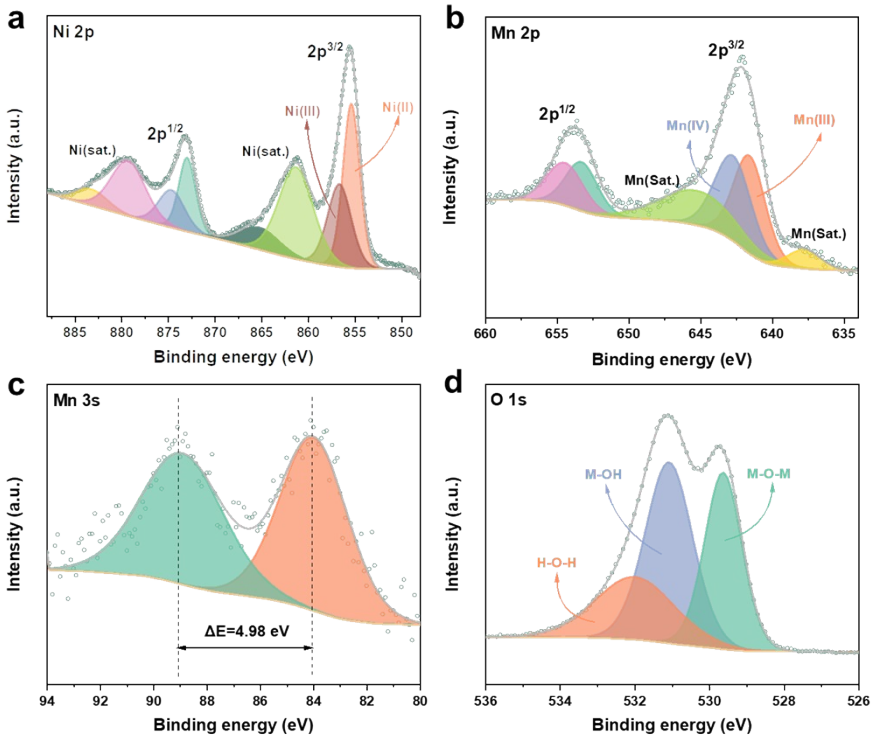

Figure S6. XPS high-resolution spectra of (a) Ni 2p, (b) Mn 2p, (c) Mn 3s and (d) O 1 s of np-NiO(MnO_x)@Ni-5.

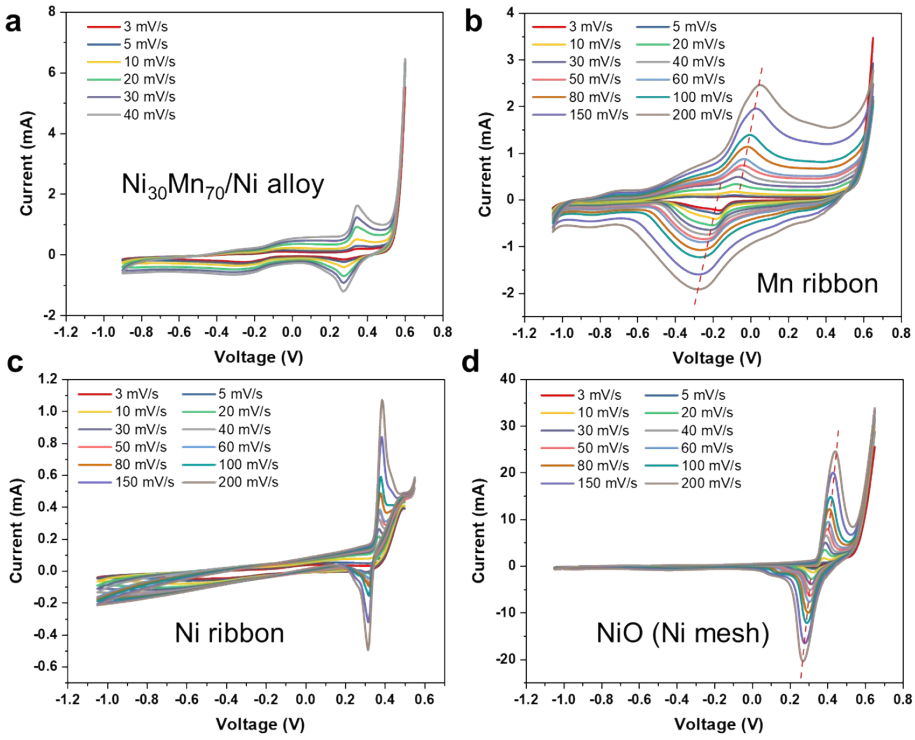

Figure S7. CV curves of pure Ni and Pure Mn potential: (a) $Ni_{30}Mn_{70}$ alloy; (b) pure Mn ribbon; (c) pure Ni ribbon; (d) commercial Ni net (oxidized at 200℃ for 3 h).

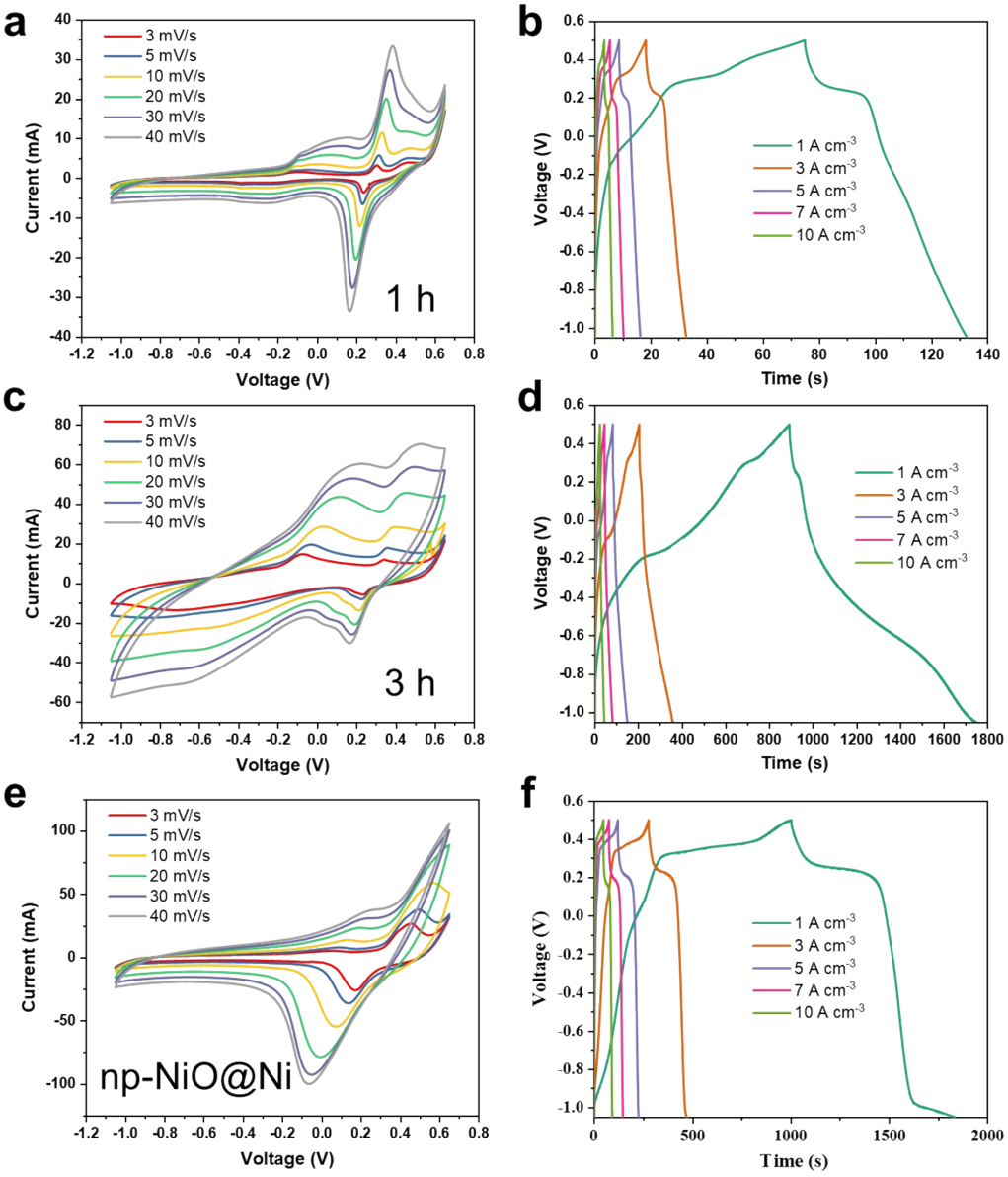

Figure S8. CV curves and GCD curves for (a-b) np-NiO(MnO_x)@Ni-1, (c-d) np-NiO(MnO_x)@Ni-3 and (e-f) np-NiO@Ni.

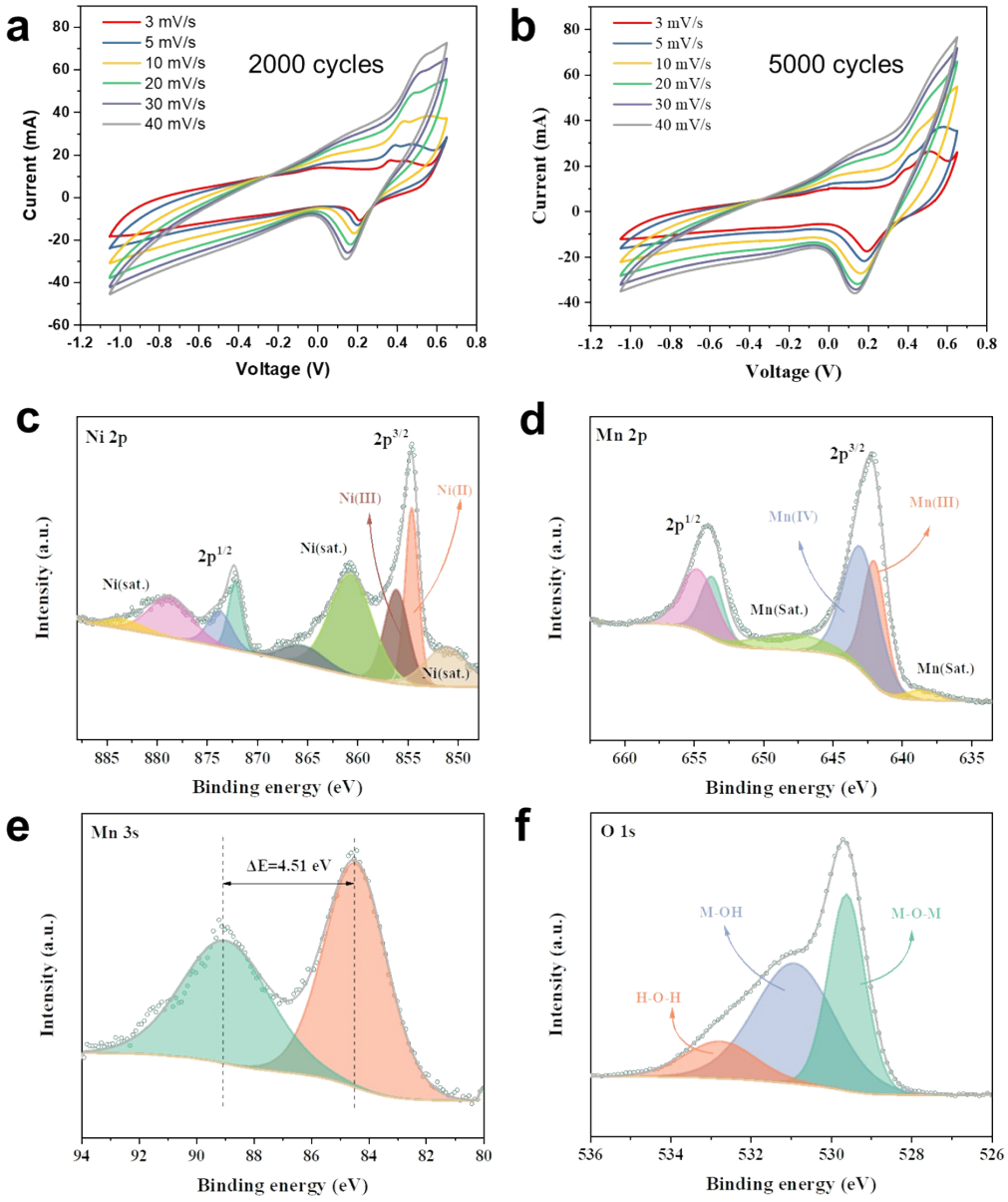

Figure S9. CV curves for (a) 2000 cycles and (b) 5000 cycles; XPS spectra for (c) Mn 2p, (d) Mn 3s, (e) Ni 2p, (f) O 1 s.

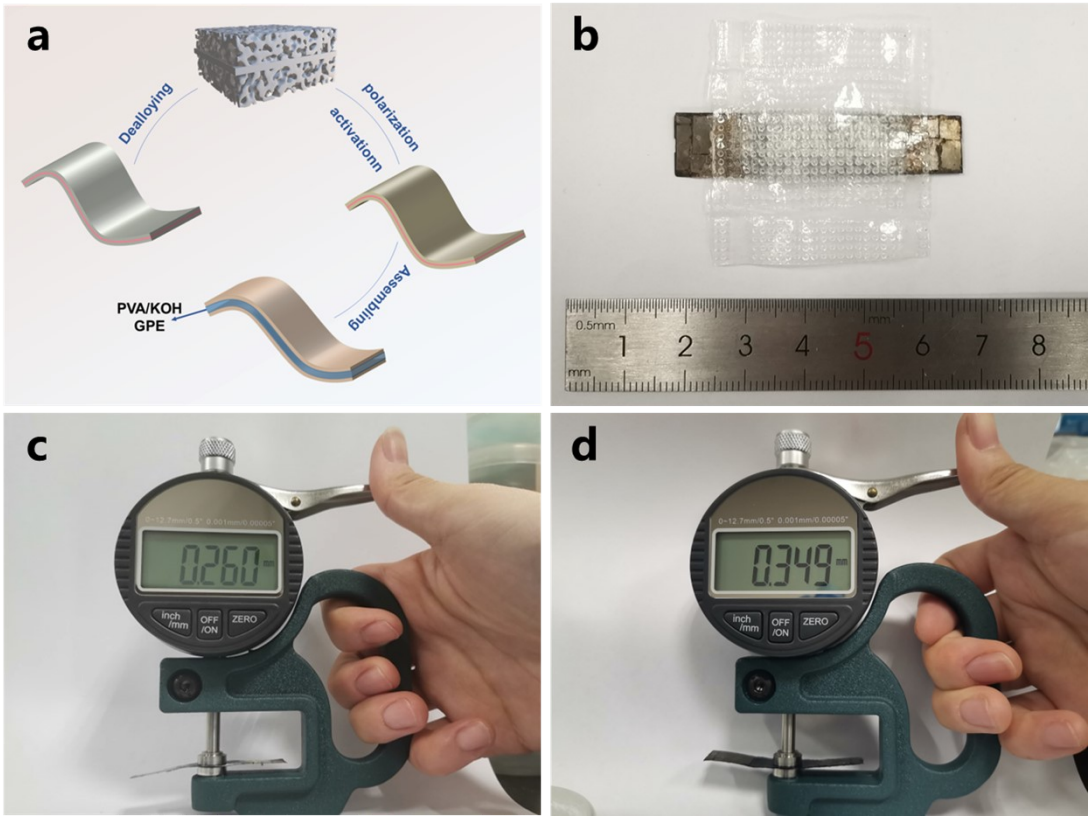

Figure S10. (a) A schematic diagram of assembling a quasi-solid-state supercapacitor; (b) digital photograph of a single SSC device; thicknesses of the quasi-solid-state supercapacitors: (c) a single SSC device and (d) a laminated SSC device.

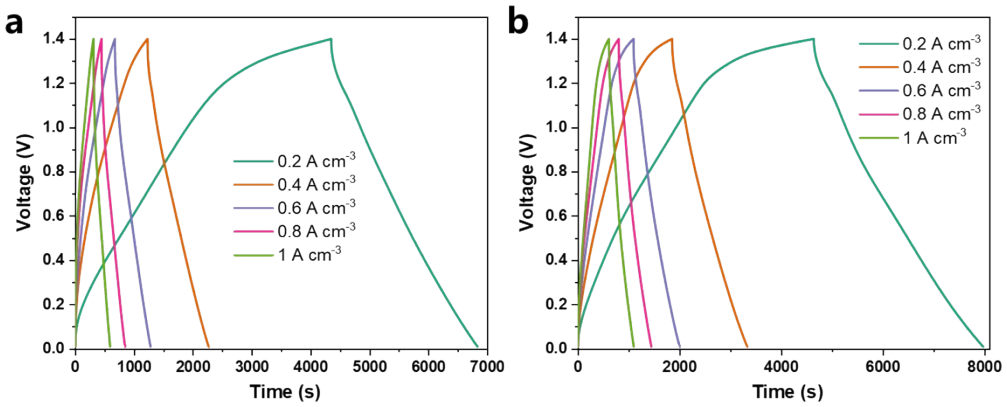

Figure S11. (a) GCD curves of a single SSC device; (b) GCD curves of a laminated SSC device.

3. Supporting Tables

Table S1. Residual content of manganese at different time of chemical dealloying.

Element (at.%)	1 h	2 h	3 h	4 h	5 h	Electrochemical dealloying
Mn	36.25	31.59	28.56	23.39	16.90	11.02
Ni	63.75	68.41	71.44	76.61	83.10	88.98
Total	100.00	100.00	100.00	100.00	100.00	100.00

Table S2. Nitrogen adsorption-desorption isotherm results of np-Ni-X (X=1, 3, 5) and np-Ni-ED precursors.

Samples	np-Ni-1	np-Ni-3	np-Ni-5	np-Ni-ED
Specific Surface Area (m^2 g^{-1})	3.387	55.700	63.047	33.647
Pore Area (m^2 g^{-1})	1.952	40.575	43.573	22.946

Table S3. The relative Ni and Mn ratio on surface in np-Ni precursors and np-NiO(MnO_x)@Ni electrodes through XPS analyses.

Element (at.%)	np-Ni-5	np-NiO(MnO_x)@Ni-5	np-Ni-ED	np-NiO@Ni
Mn	28.96	74.09	18.31	63.72
Ni	71.04	25.91	81.69	36.28
Total	100.00	100.00	100.00	100.00

Table S4. Comparison of self-discharge performance in this work and previously reported literatures.

Electrodes	Electrolyte	OCP decay	Voltage retention	Ref.
$Li_xNb_2O_5$//$Li_{2-x}Nb_2O_5$	1 M $LiPF_6$	1.00 V→0.40 V	40% after ~0.8 h	1
ZnO-Co_3O_4 SSC	PVA-Na_2SO_4	1.60 V→0.36 V	22.5% after ~8 h	2
CuO-Ni_3S_2 SSC	PVA-KOH	1.50 V→0.80 V	56% after ~2 h	3
Cu-Ni//graphite	KOH	1.00 V→0.55 V	55% after ~0.3 h	4
$Ti_3C_2T_x$ Mxene SSC	1 M KOH	0.80 V→0.40 V	50% after ~16.7 h	5
Co_3O_4@Ni_3S_4//PC	2 M KOH	1.50 V→0.75 V	50% after ~5.3 h	6
Carbon Cloth SSC	$CuCl_2$-PVA-H_2SO_4	1.00 V→0.50 V	50% after ~5.1 h	7
np-NiO(MnO_x)@Ni-5 SSC	PVA-KOH	1.40 V→0.70 V	50% after ~25 h	this work

Table S5. Comparison of electrochemical performance of different electrode have been reported.

Electrodes	Potential window	Specific capacitance	Power density (Energy density)	Cycling stability	Ref.
$NiCo_2O_4$//Fe foam	1.7 V	26.6 F cm^{-3} (2 mA cm^{-2})	14.17 mW cm^{-3} (10.68 mWh cm^{-3})	5000 (10 mA cm^{-2}, 97%)	8
MnO_2//S-MoO_{3-x}	1.8 V	6.19 F cm^{-3} (0.5 mA cm^{-1})	2.11 W cm^{-3} (2.79 mWh cm^{-3})	/	9
$ZnFe_2O_4$-NCF//$NiCo_2O_4$-NCF	1.2 V	1.97 F cm^{-3} (0.5 A g^{-1})	10 mW cm^{-3} (0.39 mWh cm^{-3})	20000 (/ , 74.5%)	10
Nb-CMO_4-C_xS_yNC//rGO/$Ti_3C_2T_x$	1.5 V	241.7 F g^{-1} (2.5 A g^{-1})	39.6 mW cm^{-3} (1.58 mWh cm^{-3})	10000 (40 A g^{-1}, 96.2%)	11
Ni-Co oxyhydroxides//AC	1.8 V	5.7 F cm^{-2} (30 mA cm^{-2})	204.1 mW cm^{-3} (19.5 mWh cm^{-3})	7000 (200 mA cm^{-2}, 91%)	12
$Ni(OH)_2$ nanowire//carbon fiber	1.5 V	35.67 F cm^{-2} (0.1 mA)	1.6 W cm^{-3} (2.16 mWh cm^{-3})	10000 (10 A cm^{-3}, 70%)	13
Ni/MnO_2-FP//Ni/AC-FP	2.5 V	1.4 F cm^{-3} (2.5 mA cm^{-3})	2.5 mW cm^{-3} (0.78 mWh cm^{-3})	1000 (20 mA cm^{-2}, 85.1%)	14
MnO_2/PEDOT-PSS//OMC	1.8 V	23.4 F cm^{-3} (0.085 A cm^{-3})	0.03 W cm^{-3} (11.3 mWh cm^{-3})	1000 (20 mA cm^{-2}, 85.1%)	15
Cu-CuO@CoFe-LDH//Cu-AC	1.2 V	9.38 F cm^{-3} (0.25 A cm^{-3})	914.5 mW cm^{-3} (1.857 mWh cm^{-3})	2000 (0.5 A cm^{-3}, 99.5%)	16
Ni-doped MnO_2@CC SSC	1.2 V	71.54 mF cm^{-2} (2 mA cm^{-3})	31.43 mW cm^{-3} (0.6871 mWh cm^{-3})	/	17
np-NiO(MnO_x)@Ni-5 SSC	1.5 V	138.36 F cm^{-3} (0.2 A cm^{-3})	3253.68 mW cm^{-3} (8.07 mWh cm^{-3})	5000 (10 A cm^{-3}, 91%)	**this work**

References

1. X. Yan, S. Jing, T. Li, Y. Xiong, T. Hu, Z. Wang and X. Ge, *Chemical Engineering Journal*, 2022, **450**.
2. R. K. Mishra, G. J. Choi, H. J. Choi, J. Singh, F. S. Mirsafi, H.-G. Rubahn, Y. K. Mishra, S. H. Lee and J. S. Gwag, *Chemical Engineering Journal*, 2022, **427**.
3. D. Mishra, S. Kim, N. Kumar, M. Krishnaiah and S. H. Jin, *Journal of Materials Science & Technology*, 2023, **147**, 77-90.
4. A. Yavuz, M. Artan and N. F. Yilmaz, *Journal of Physics and Chemistry of Solids*, 2022, **169**.
5. S. Pu, Z. Wang, Y. Xie, J. Fan, Z. Xu, Y. Wang, H. He, X. Zhang, W. Yang and H. Zhang, *Advanced Functional Materials*, 2022, **33**.
6. J. Chang, S. Zang, Y. Wang, C. Chen, D. Wu, F. Xu, K. Jiang, Z. Bai and Z. Gao, *Electrochimica Acta*, 2020, **353**.
7. H. Wang, J. Chen, R. Fan and Y. Wang, *Sustainable Energy & Fuels*, 2018, **2**, 2727-2732.
8. C. Zhang, L. Hou, W. Yang, S. Du, B. Jiang, H. Bai, Z. Li, C. Wang, F. Yang and Y. Li, *Chemical Engineering Journal*, 2023, **467**.
9. S. Liu, C. Xu, H. Yang, G. Qian, S. Hua, J. Liu, X. Zheng and X. Lu, *Small*, 2020, **16**.
10. B. H. Xiao, R. T. Lin, K. Xiao and Z. Q. Liu, *Journal of Power Sources*, 2022, **530**.
11. A. M. Patil, S. Moon, Y. Seo, S. B. Roy, A. A. Jadhav, D. P. Dubal, K. Kang and S. C. Jun, *Small*, 2023, **19**, e2205491.
12. X. Ren, M. Li, L. Qiu, X. Guo, F. Tian, G. Han, W. Yang and Y. Yu, *Journal of Materials Chemistry A*, 2023, **11**, 5754-5765.
13. X. Dong, Z. Guo, Y. Song, M. Hou, J. Wang, Y. Wang and Y. Xia, *Advanced Functional Materials*, 2014, **24**, 3405-3412.
14. L. Zhang, P. Zhu, F. Zhou, W. Zeng, H. Su, G. Li, J. Gao, R. Sun and C.-p. Wong, *ACS Nano*, 2015, **10**, 1273-1282.
15. X. Cheng, J. Zhang, J. Ren, N. Liu, P. Chen, Y. Zhang, J. Deng, Y. Wang and H. Peng, *The Journal of Physical Chemistry C*, 2016, **120**, 9685-9691.
16. Z. Li, M. Shao, L. Zhou, R. Zhang, C. Zhang, J. Han, M. Wei, D. G. Evans and X. Duan, *Nano Energy*, 2016, **20**, 294-304.
17. R. Zhong, M. Xu, N. Fu, R. Liu, A. a. Zhou, X. Wang and Z. Yang, *Electrochimica Acta*, 2020, **348**.